13. Smith, D. K. & Cann, J. R. *Nature* **348,** 152–155 (1990).
14. Smith, D. K. & Cann, J. R. *J. geophys. Res.* **97,** 1645–1658 (1992).
15. Macdonald, K. C. *et al. Nature* **335,** 217–225 (1988).
16. Heezen, B. C. & Tharp, M. *Geol. Soc. Am. Map* (Geol. Soc. Am., Boulder, 1957).
17. Aumento, F., Loncarevic, B. D. & Ross, D. I. *Phil. Trans. R. Soc.* **268,** 623–650 (1971).
18. Heirtzler, J. R. & van Andel, Tj. H. *Geol. Soc. Am. Bull.* **88,** 481–487 (1977).
19. Crane, K. & Ballard, R. D. *J. geophys. Res.* **86,** 5112–5124 (1981).
20. Scott, R. B., Rona, P. A., McGregor, B. A. & Scott, M. R. *Nature* **251,** 301–302 (1974).
21. Phillips, J. D. & Fleming, H. S. *Geol. Soc. Am. Maps MC-19* (Geol. Soc. Am., Boulder, 1978).
22. Purdy, G. M., Sempere, J.-C., Schouten, H., Dubois, D. L. & Goldsmith, R. *Mar. geophys. Res.* **12,** 247–252 (1990).
23. Ramberg, I. B., Gray, D. F. & Raynolds, R. G. H. *Geol. Soc. Am. Bull.* **88,** 609–620 (1977).
24. Crane, K. *Earth planet. Sci. Lett.* **72,** 405–414 (1985).
25. Schouten, H., Klitgord, K. D. & Whitehead, J. A. *Nature* **317,** 225–229 (1985).
26. Purdy, G. M. & Detrick, R. S. *J. geophys. Res.* **91,** 3739–3762 (1986).
27. Kuo, B. Y. & Forsyth, D. W. *Mar. geophys. Res.* **10,** 205–232 (1988).
28. Lin, J., Purdy, G. M., Schouten, H., Sempere, J.-C. & Zervas, C. *Nature* **344,** 627–632 (1990).
29. Shaw, P. R. *Nature* **358,** 490–493 (1992).
30. Kong, L. S., Detrick, R. S., Fox, P. J., Mayer, L. A. & Ryan, W. B. F. *Mar. geophys. Res.* **10,** 59–90 (1988).
31. Brown, J. R. & Karson, J. A. *Mar. geophys. Res.* **10,** 109–138 (1988).
32. Gente, P., Mevel, C., Auzende, J. M., Karson, J. A. & Fouquet, Y. *Tectonophysics* **190,** 1–29 (1991).
33. Macdonald, K. C. & Luyendyk, B. P. *Geol. Soc. Am. Bull.* **88,** 621–636 (1977).
34. Luyendyk, B. P. & Macdonald, K. C. *Geol. Soc. Am. Bull.* **88,** 648–663 (1977).
35. Bonatti, E. & Harrison, C. G. A. *J. geophys. Res.* **93,** 2967–2980 (1988).
36. Bryan, W. B. & Moore, J. G. *Geol. Soc. Am. Bull.* **88,** 556–570 (1977).
37. Atwater, T. in *Deep Drilling Results in the Atlantic Ocean: Ocean Crust* Vol. 2 (eds Talwani, M., Harrison, C. G. & Hayes, D. E.) 33–42 (Am. geophys. Un., Washington DC, 1979).
38. Zonenshain, L. P. *et al. Tectonophysics* **159,** 1–23 (1989).
39. Detrick, R. S. *et al. Nature* **326,** 35–41 (1987).
40. Herron, T. J., Ludwig, W. J., Stoffa, P. L., Kan, T. K. & Buhl, P. *J. geophys. Res.* **83,** 798–804 (1978).
41. Sinton, J. M. & Detrick, R. S. *Mar. geophys. Res.* **97,** 197–216 (1992).
42. Whitmarsh, R. B. *Nature* **246,** 297–299 (1973).
43. Fowler, C. M. & Keen, C. E. *Geophys. J. R. astr. Soc.* **56,** 219–226 (1979).
44. Toomey, D. R., Solomon, S. C. & Purdy, G. M. *J. geophys. Res.* **93,** 9093–9112 (1988).
45. Huang, P. Y. & Solomon, S. C. *J. geophys. Res.* **93,** 13445–13477 (1988).
46. Detrick, R. S., Mutter, J. C., Buhl, P. & Kim, I. I. *Nature* **347,** 61–64 (1990).
47. Kong, L. S., Solomon, S. C. & Purdy, G. M. *J. geophys. Res.* **97,** 1659–1685 (1992).
48. Nisbet, E. G. & Fowler, C. M. R. *Geophys. J. R. astr. Soc.* **54,** 631–660 (1978).
49. Harper, G. *Tectonics* **4,** 395–409 (1985).
50. Chen, Y. & Jason Morgan, W. *J. geophys. Res.* **95,** 17583–17604 (1990).
51. Phipps Morgan, J. & Chen, Y. J. *J. geophys. Res.* **98,** 6283–6297 (1993).
52. Daly, R. A. *Igneous Rocks and the Depths of the Earth* (McGraw-Hill, New York, 1933).
53. Barone, A. M. & Ryan, W. B. F. *J. geophys. Res.* **95,** 10801–10827 (1990).
54. Ryan, M. P. in *Magmatic Processes: Physiochemical Principles* (ed. Mysen, B. O.) 259–287 (Geochem. Soc. spec. Publ., University Park, Pennsylvania, 1987).
55. Wilson, L., Head, H. W. & Parfitt, E. A. *Geophys. Res. Lett.* **19,** 1395–1398 (1992).
56. Tilling, R. I. & Dvorak, J. J. *Nature* **363,** 125–132 (1993).
57. Becker, K. *Init. Rep. DSDP Leg* **83,** 419–427 (1985).
58. Becker, K., Langseth, M. G., Von Herzen, R. P., Anderson, R. N. & Hobart, M. A. *Init. Rep. DSDP Leg* **83,** 405–418 (1985).
59. Gass, I. G. & Smewing, J. D. in *The Sea 7: The Oceanic Lithosphere* (ed. Emiliani, C.) 339–362 (Wiley, New York, 1981).
60. Harper, G. *Geol. Soc. Am. Bull.* **95,** 1009–1026 (1984).
61. Hooft, E. E. & Detrick, R. S. *Geophys. Res. Lett.* **20,** 423–426 (1993).
62. Macdonald, G. A. & Abbott, A. T. *Volcanoes in the Sea* (Univ. Hawaii Press, Honolulu, 1970).
63. Walker, G. P. L. *Leicester Lit. Phil. Soc. Trans.* **51,** 25–40 (1964).
64. Whitehead, J. A. & Helfrich, K. R. *J. geophys. Res.* **96,** 4145–4155 (1991).
65. Gass, I. G. *Geol. Surv. Cyprus Mem.* **4,** 1–116 (1960).
66. Gass, I. G. *Nature* **220,** 39–42 (1968).
67. Moores, E. M. & Vine, F. J. *Phil. Trans. R. Soc.* A**268,** 443–466 (1971).
68. Wilson, R. A. M. *Geol. Surv. Cyprus Mem.* **1,** 1–135 (1959).
69. Auzende, J.-M. *et al. Nature* **337,** 726–729 (1989).
70. Humphris, S. E., Bryan, W. B., Thompson, G. & Autio, L. K. *Proc. ODP Sci. Res.* **106/109** 67–84 (1990).
71. Perry, F. V., Baldridge, W. S., DePaolo, D. J. & Shafiqullah, M. *J. geophys. Res.* **95,** 19327–19348 (1990).
72. Cann, J. R. *Geophys. J. R. astr. Soc.* **39,** 169–187 (1974).
73. Atwater, T. & Mudie, J. D. *J. geophys. Res.* **78,** 8665–8686 (1973).
74. Kidd, R. G. W. *Geophys. J. R. astr. Soc.* **50,** 149–183 (1977).
75. Solomon, S. C. & Toomey, D. R. *A. Rev. Earth planet. Sci.* **20,** 329–364 (1992).
76. Gentre, P. *et al. C.r. Seanc. Acad. Sci., Paris* **308,** 1781–1788 (1989).
77. Eberhart, G. L., Rona, P. A. & Honnorez, J. *Mar. geophys. Res.* **10,** 233–259 (1988).
78. Shaw, P. R. & Lin, J. *J. geophys. Res.* (in the press).

ACKNOWLEDGEMENTS. We thank the master, crew and scientific party of RV *Charles Darwin*, and the Institute of Oceanographic Sciences, Deacon Lab., for providing and supporting TOBI at sea. Funding was from the NERC and the US Office of Naval Research.

A search for life on Earth from the Galileo spacecraft

Carl Sagan*, W. Reid Thompson*, Robert Carlson†, Donald Gurnett‡ & Charles Hord§

* Laboratory for Planetary Studies, Cornell University, Ithaca, New York 14853, USA
† Atmospheric and Cometary Sciences Section, Jet Propulsion Laboratory, Pasadena, California 91109, USA
‡ Department of Physics and Astronomy, University of Iowa, Iowa City, Iowa 52242-1479, USA
§ Laboratory for Atmospheric and Space Physics, University of Colorado, Boulder, Colorado 80309, USA

In its December 1990 fly-by of Earth, the Galileo spacecraft found evidence of abundant gaseous oxygen, a widely distributed surface pigment with a sharp absorption edge in the red part of the visible spectrum, and atmospheric methane in extreme thermodynamic disequilibrium; together, these are strongly suggestive of life on Earth. Moreover, the presence of narrow-band, pulsed, amplitude-modulated radio transmission seems uniquely attributable to intelligence. These observations constitute a control experiment for the search for extraterrestrial life by modern interplanetary spacecraft.

At ranges varying from ~100 km to ~100,000 km, spacecraft have now flown by more than 60 planets, satellites, comets and asteroids. They have been equipped variously with imaging systems, photometric and spectrometric instruments extending from ultraviolet to kilometre wavelengths, magnetometers and charged-particle detectors. In none of these encounters has compelling, or even strongly suggestive, evidence for extraterrestrial life been found. For the Moon, Venus and Mars, orbiter and lander observations confirm the conclusion from fly-by spacecraft. Still, extraterrestrial life, if it exists, might be quite unlike the forms of life with which we are familiar, or present only marginally. The most elementary test of these techniques—the detection of life on Earth by such an instrumented fly-by spacecraft—had, until recently, never been attempted.

Galileo is a single-launch Jupiter orbiter and entry probe currently in interplanetary space and scheduled to arrive in the Jupiter system in December 1995. It could not be sent directly to Jupiter; instead, the mission incorporated two close gravitational assists at the Earth and one at Venus. This greatly lengthened the transit time, but it also permitted close observations of the Earth. The

Galileo instruments were not designed for an Earth encounter mission, so an appropriate control experiment has fortuitously been arranged: a search for life on Earth with a typical modern planetary probe.

Closest approach to Earth in the 8 December 1990 encounter was 960 km over the Caribbean Sea. The Earth was approached from its night side, so all data in reflected light were acquired post-encounter. Evidence relevant to the search for life was obtained with the near-infrared mapping spectrometer (NIMS), the ultraviolet spectrometer (UVS), the solid-state imaging system (SSI), and the plasma wave spectrometer (PWS). These instruments are described in refs 1–4, respectively. Because of the high encounter velocity, most NIMS and SSI data were obtained 2 hours to 3.5 days after closest approach.

In what follows, we do not assume properties of life otherwise known on Earth, but instead attempt to derive our conclusions from Galileo data and first principles alone. We compare these conclusions with ground-based and low-altitude measurements that we describe, collectively, as the 'ground-truth Earth'. A necessary but not sufficient condition for the presence of life is a marked departure from thermodynamic equilibrium[5–8]. Once candidate disequilibria are identified, alternative explanations must be eliminated. Life is the hypothesis of last resort. As an analogy, mountains are in mechanical disequilibrium, given the Earth's erosional environment, but orogenic processes build mountains faster than wind, water and plate tectonics destroy them. Ozone is in substantial thermodynamic disequilibrium in the Earth's atmosphere, but this is driven by solar ultraviolet (UV) photochemistry. Bursts of high-brightness-temperature kilometre-wave radiation occur in the Earth's auroral zones, but are pumped by the interaction of the solar wind with the Earth's magnetosphere. No biological explanations of these disequilibrium phenomena need to be sought. As we will show, however, Galileo found such profound departures from equilibrium that the presence of life seems the most probable cause.

Chemistry

NIMS spectral and radiometric measurements indicate the presence of water in several forms. Spectra of Antarctica[9] show distinctive features due to condensed water, which are broadened and shifted to longer wavelengths compared to gas-phase features. The radiometric temperatures (~−30 °C) indicate ice, and analysis of the spectra[9] give snow grain sizes of 50–200 μm. This ice and snow cover occurs on continental scale around the South Pole.

At higher latitudes are extensive areas with higher, nearly uniform temperatures just at, or slightly above, the melting point of water. In particular, the radiometric temperatures measured at 5 μm, uncorrected for atmospheric absorption, are ~−3 °C at high southern latitudes, increasing to 8–18 °C at midlatitudes. The average 1 μm albedo of these extensive areas is ~4%, much smaller than the albedos of snow, clouds and rocky surfaces, but consistent with the low diffuse reflectance of dielectric liquid surfaces, including water. In many of the NIMS images, greatly enhanced specular reflection is observed[10]—implying the existence of large areas that are macroscopically smooth and homogenous (that is, not granular) and most easily explained by the presence of liquid surfaces of oceanic dimensions. Evidence of gas-phase H_2O is found over the entire planet. Representative NIMS infrared spectra in the 0.7–1.0 μm range, and in the 2.4–5.2 μm range, are shown in Fig. 1. They were obtained over a fairly clear area in the eastern Pacific, north of Borneo. Analysis[10] of the vibration–rotation bands of water vapour gives typical abundances of ~1,000 parts per million (p.p.m.) or ~0.6 g cm^{-2}. The observed high humidities, found over most of the planet, along with the preceding discussion, imply that the oceans are composed of liquid water.

Spectral data aside, from the albedo and heliocentric distance of the Earth alone it follows that the equilibrium temperature of the planet is only 20 °C or so below the freezing point of water—so that even a modest greenhouse effect would bring temperatures high enough that water, a cosmically abundant molecule, could exist in all three of its phases. Abundant surface liquid water is seen nowhere else in the contemporary Solar System. The dielectric constant, solvation properties, heat capacity, and temperature range of the liquid state are among the nonparochial reasons that water seems an ideal medium for life[11].

Figure 1 is notable for the presence of the A band of molecular oxygen at 0.76 μm. This transition is spin-forbidden, and the strength of the feature indicates ~200 g cm^{-2} of O_2 (Table 1). So large an abundance of O_2 is also unique among all the worlds

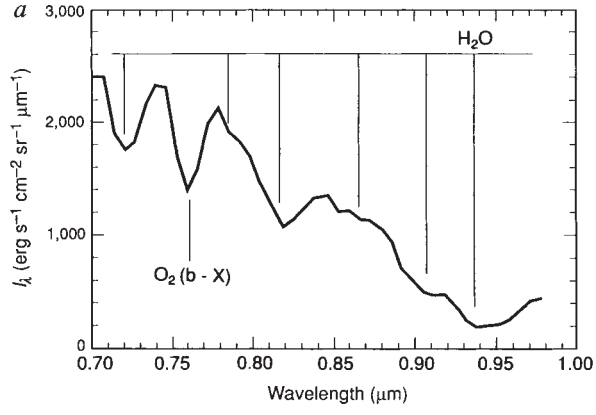

FIG. 1 *a*, Galileo long-wavelength-visible and near-infrared spectra of the Earth over a relatively cloud-free region of the Pacific Ocean, north of Borneo. The incidence and emission angles are 77° and 57° respectively. The ($b'\Sigma_g^+$—$X^3\Sigma_g^-$) 0–0 band of O_2 at 0.76 μm is evident, along with a number of H_2O features. Using several cloud-free regions of varying airmass, we estimate an O_2 vertical column density of 1.5 km-amagat ± 25%. *b* and *c*, Infrared spectra of the Earth in the 2.4–5.2 μm region. The strong υ_3 CO_2 band is seen at the 4.3 μm, and water vapour bands are found, but not indicated, in the 3.0 μm region. The υ_3 band of nitrous oxide, N_2O, is apparent at the edge of the CO_2 band near 4.5 μm, and N_2O combination bands are also seen near 4.0 μm. The methane (0010) vibrational transition is evident at 3.31 μm. A crude estimate[10] of the CH_4 and N_2O column abundances is, for both species, of the order of 1 cm-amagat (≡1 cm path at STP).

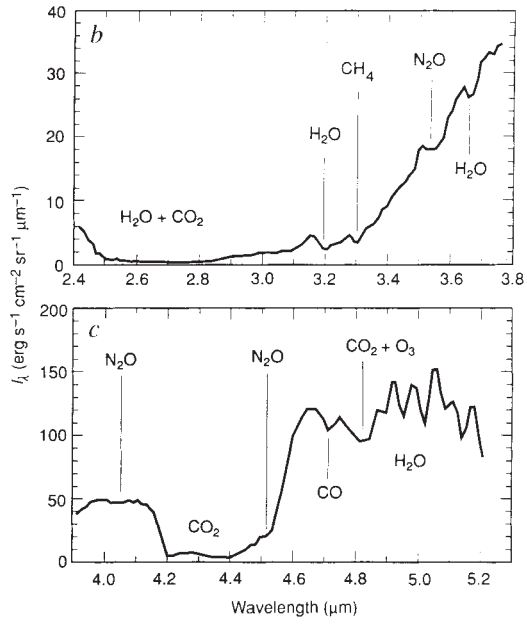

TABLE 1 Constituents of the Earth's atmosphere (volume mixing ratios)

Molecule	Standard abundance (ground-truth Earth)	Galileo value*	Thermodynamic equilibrium value Estimate 1†	Estimate 2‡
N_2	0.78		0.78	
O_2	0.21	0.19 ± 0.05	0.21§	
H_2O	0.03–0.001	0.01–0.001	0.03–0.001	
Ar	9×10^{-3}		9×10^{-3}	
CO_2	3.5×10^{-4}	$5 \pm 2.5 \times 10^{-4}$	3.5×10^{-4}	
CH_4	1.6×10^{-6}	$3 \pm 1.5 \times 10^{-6}$	$< 10^{-35}$	10^{-145}
N_2O	3×10^{-7}	$\sim 10^{-6}$	2×10^{-20}	2×10^{-19}
O_3	10^{-7}–10^{-8}	$> 10^{-8}$	6×10^{-32}	3×10^{-30}

* Galileo values for O_2, CH_4 and N_2O from NIMS data; O_3 estimate from UVS data.

† From ref. 16 (P, 1 bar; T, 280 K).

‡ From ref. 17 (P, 1 bar; T, 298 K).

§ The observed value; it is in thermodynamic equilibrium only if the under-oxidized state of the Earth's crust is neglected.

in the Solar System. Oxygen can be generated by the UV photodissociation of water and the subsequent Jeans escape of H to space. But can the accumulation of so much O_2 over geological time be understood?

Certainly, Venus and Mars—where atmospheric water vapour is being UV photodissociated—display very low O_2 abundances, <1 and $\sim 10^{-3}$ p.p.m., respectively[12,13], despite large quantities of water lost through photodissociation and atmospheric escape of H. But a real understanding of the Earth's steady-state O_2 abundance requires at the least knowledge of the oxidation state of the surface, surface erosion rates, and temperatures at the tropopause, the mesopause and the exobase. Galileo did not provide this data set. Even if it had, we could not be confident that present circumstances are typical of Earth history. An upper bound on the UV generation rate of O_2 is set by the photon-limited water photolysis rate, $\sim 10^{13}\,cm^{-2}\,s^{-1}$ on the ground-truth Earth[14]—which yields the present O_2 abundance in $<10^5$ yr. If instead we use the ground-truth present H escape flux[14] (which is H_2O diffusion-limited) and assume that all the H atoms are H_2O-derived, the present O_2 abundance would require several times the age of the Earth to accumulate. If there is substantial oxidation of the crust, these timescales will be longer. But the lack of impact craters in Galileo imagery, and pervasive wind and water on Earth suggest continuing exposure of fresh, oxidizable regolith. Accordingly, oxidation of the Earth's crust should be more extensive than on Venus and Mars, and yet these planets have much less atmospheric O_2. Galileo's observations of O_2 thus at least raise our suspicions about the presence of life. If detailed modelling showed solar UV to be insufficient, a process seems needed whereby the much more abundant, but much less energetic visible light photons are used in series for

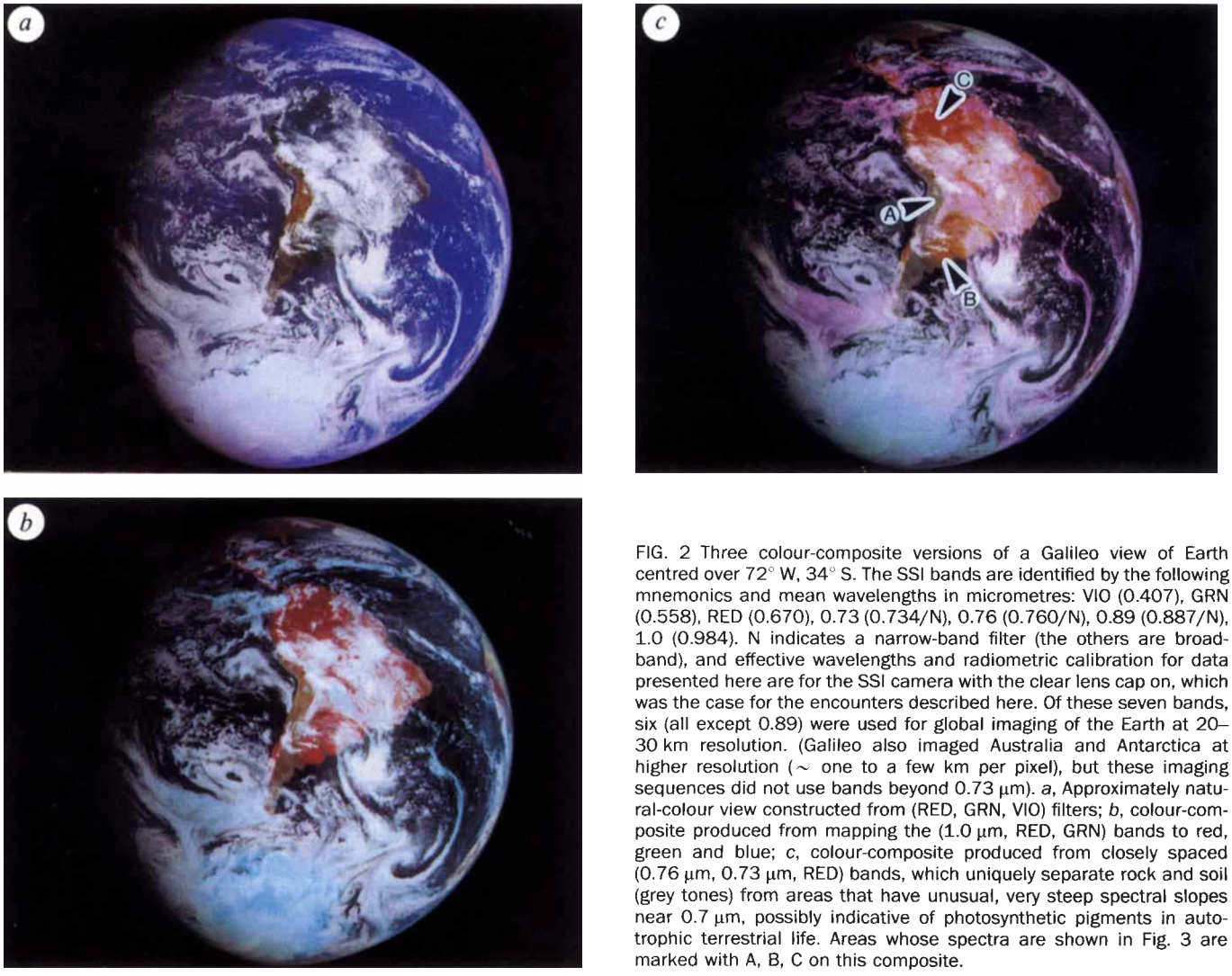

FIG. 2 Three colour-composite versions of a Galileo view of Earth centred over 72° W, 34° S. The SSI bands are identified by the following mnemonics and mean wavelengths in micrometres: VIO (0.407), GRN (0.558), RED (0.670), 0.73 (0.734/N), 0.76 (0.760/N), 0.89 (0.887/N), 1.0 (0.984). N indicates a narrow-band filter (the others are broad-band), and effective wavelengths and radiometric calibration for data presented here are for the SSI camera with the clear lens cap on, which was the case for the encounters described here. Of these seven bands, six (all except 0.89) were used for global imaging of the Earth at 20–30 km resolution. (Galileo also imaged Australia and Antarctica at higher resolution ($\sim$ one to a few km per pixel), but these imaging sequences did not use bands beyond 0.73 μm). *a*, Approximately natural-colour view constructed from (RED, GRN, VIO) filters; *b*, colour-composite produced from mapping the (1.0 μm, RED, GRN) bands to red, green and blue; *c*, colour-composite produced from closely spaced (0.76 μm, 0.73 μm, RED) bands, which uniquely separate rock and soil (grey tones) from areas that have unusual, very steep spectral slopes near 0.7 μm, possibly indicative of photosynthetic pigments in autotrophic terrestrial life. Areas whose spectra are shown in Fig. 3 are marked with A, B, C on this composite.

H_2O photodissociation (at least two visible photons would be needed per photodissociation event). Apparently, only biological systems can accomplish this.

In Fig. 1*b* and *c*, the presence of carbon dioxide, methane, nitrous oxide and ozone are indicated. All are greenhouse gasses; together with water vapour, they mainly account for the discrepancy between the equilibrium and measured radiometric temperatures of the Earth's surface.

From straightforward photochemical theory it follows[15] that one consequence of the high oxygen abundance is a stratospheric ozone layer opaque in the middle UV. Even a quick look at the Galileo UVS raw data shows the strong Hartley bands of O_3 at wavelengths greater than 0.21 μm in the spectrum of the Earth but not of Venus. (O_3 absorption is also found in NIMS infrared spectra.) The presence of disequilibrium O_3 is not in itself a sign of life, because UV photochemistry is a disequilibrium process, but the photochemical abundance of O_3 is related approximately logarithmically to the O_2 abundance, so the observed quantity of O_3 does imply a substantial abundance of O_2. Therefore a train of argument may exist[15] from abundant O_3 to abundant O_2 to life. The Hartley bands provide substantial optical depth at wavelengths less than ~0.3 μm, suggesting that in addition to the oceans (where life could be protected at depth from UV radiation), life on the land is also possible provided structural molecular bond strengths exceed ~50 kcal mol^{-1}. In this category fall a large number of organic functional groups, including C–C (70–130 kcal mol^{-1}), C–H (80–110), C–O (~90) and C–N (80–100). Corresponding multiple bonds are even stronger. Of course this is not, by itself, an argument for organic biochemistry on Earth.

The agreement of ground-truth atmospheric abundances with those determined by Galileo is reasonably good (Table 1). Also shown in Table 1 are two independent estimates[16,17], made 25 years apart, of the thermodynamic equilibrium abundances expected of minor constituents in the observed excess of O_2. Such calculations are characteristically performed by minimizing the free energy of the system while simultaneously satisfying the equilibrium constants of all known reactions of all known reactants. This approach is less vulnerable to unknown reaction pathways or erroneous rate constants than is absolute reaction rate kinetics. But it is an idealization at best, because thermodynamic equilibrium may not be achieved in the age of the Solar System, and because there are prominent nonequilibrium processes including photochemistry and biology. Ozone is present at more than 20 orders of magnitude above its thermodynamic expectation value, but, as noted above, this disequilibrium is not considered evidence for life because a UV photochemical pathway from O_2 to this O_3 abundance is well known.

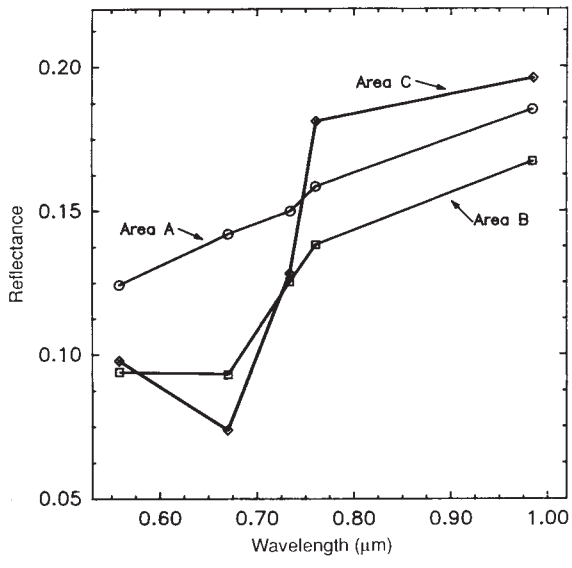

FIG. 3 Representative spectra from three areas on the land surface (see Fig. 2c). A gently sloping spectrum (circles, Area A) is consistent with any of several types of rock or soil. An intermediate spectrum (squares, Area B) shows some evidence of an absorption band near 0.67 μm (RED). Substantial areas on the surface have an unusual spectrum (diamonds, Area C) with a strong absorption in the RED band and a steep band edge just beyond 0.7 μm. This spectrum is inconsistent with all likely rock and soil types, and is plausibly associated with photosynthetic pigments (see text).

The circumstance of methane is different. It is oxidized quickly to CO_2 and H_2O, and at thermodynamic equilibrium there should not be a single methane molecule in the Earth's atmosphere[16,17]. The disparity between observation and thermodynamic equilibrium is about 140 orders of magnitude. Clearly there is some mechanism that pumps CH_4 into the Earth's atmosphere so rapidly that substantial steady-state abundances accrue before oxidation can keep pace. It has long been suggested that an extreme disequilibrium abundance of a reduced gas such as CH_4 in an O_2-rich atmosphere could be evidence for life on Earth[6–8,16]. The total emission flux of CH_4 into the atmosphere of the ground-truth Earth from all sources[18] required to sustain the steady state abundance is 500 ± 100 Tg yr^{-1} (where 1 Tg is 10^{12} g), or ~10^{-4} g cm^{-2} yr^{-1}, an oxidation of all atmospheric CH_4 roughly every decade. Conceivably, methane could be injected into the Earth's atmosphere by other means (for example, the decomposition of prebiological organic matter) but so large a rate of injection, corresponding to ~1 bar of CH_4 after only 10^7 yr, seems highly implausible. Oxidation of such organic matter has certainly gone to completion on, for example, Venus. In fact, on the ground-truth Earth the contribution of volcanos, fumaroles, and earthquakes to atmospheric CH_4 is negligible[18]. About half the annual CH_4 injection is thought to arise from natural systems (methane bacteria and so on) and approximately half is anthropogenic; rice cultivation, biomass burning and flatulence from domesticated ruminants are among the principal sources[18]. All these sources are biological, including those deriving from fossil fuels. Thus the disequilibrium abundance of CH_4 in the Earth's oxidizing atmosphere is found by ground-based observations to be indeed caused by biology, as naive consideration of the Galileo data would suggest. It is also evidence that organic chemistry plays some role in life on Earth.

The presence of nitrous oxide (N_2O) in the atmosphere at high disequilibrium abundances is another indicator of biological processes. Nitrous oxide is partly lost to photodissociation, with an atmospheric lifetime[19] of about 50 years. Although there are non-biological mechanisms for producing N_2O (for example lightning), the major source of N_2O on the ground-truth Earth is nitrogen-fixing bacteria and algae that convert soil and oceanic nitrate (NO_3^-) to N_2 and N_2O.

Imaging

A typical Galileo image of the Earth shows continents, oceans, the Antarctic polar cap and a highly time-variable configuration of clouds. The six bands used in SSI global images can be combined in various ways to visualize specific spectral contrasts in the clouds or on the surface. Of the many possibilities, three categories of band combinations prove most informative. First is (RED, GRN, VIO) (equivalent wavelengths 0.670, 0.558 and 0.407 μm respectively), which gives an approximately natural colour view (Fig. 2*a*). Large expanses of blue ocean and apparent coastlines are present, and close examination of the images shows a region of specular reflection in ocean but not on land. Clouds cover much of the land surface, but in clear areas extreme albedo contrasts are seen. The lighter areas have a colour compatible with mineral soils, while a greenish tint can be perceived in the darkest areas.

Second, we may translate (1.0, RED, GRN) (equivalent wavelength of 1.0 is 0.984 μm) bands to red, green and blue, respectively, in a false-colour image (Fig. 2*b*). This version reveals two kinds of sharp spectral contrasts. First, the cyan colour of the bright polar cap is caused by absorption in the 1.0 μm band, which confirms its H_2O-ice composition, and second, some land areas appear bright red, indicating a high albedo at 1.0 μm along with a low albedo in the visible spectrum (especially RED). Even without additional spectral information, a GRN/RED/1.0 signature so extreme is inconsistent with most dry or hydrated rocks or soils that might be expected on the surface of a terrestrial planet.

Using the 0.73 and 0.76 μm bands deepens the mystery. Figure 3 shows average mean spectra for three classes of land surface. (VIO is not plotted because of strong, differential atmospheric scattering corrections that are not fully modelled). The spectrum of area A (circles) has a gentle slope that rises in brightness uniformly from GRN to 1.0 μm, consistent with a variety of dark rock or mineral-soil surfaces. The spectrum of area B, an intermediate-albedo area, shows an absorption centred at RED. Although such areas are common on the surface, no common igneous, altered igneous, or sedimentary rock/soil surface displays such a signature[20]. The spectrum of area C is from a large low-albedo area in the northern part of the continent. Its very unusual spectrum has a strong absorption in the visible spectrum and a very steep spectral slope from 0.67 (RED) to 0.76 μm.

The third category of colour composite uses three closely spaced bands (0.76, 0.73, RED), and emphasizes strong spectral slopes over this narrow wavelength range (0.67–0.76 μm) (Fig. 2*c*). Areas that have gently sloped spectra consistent with plausible rocks and soils appear grey here, whereas areas dominated by the unusual surface material with a strong absorption edge near 0.7 μm appear in greenish-yellow/orange hues. (The only other substantial contrast are the magenta areas in clouds, due to the 0.73 μm water-vapour band.)

These spectra cannot by uniquely interpreted; however, because they are inconsistent with any known rock or soil types on terrestrial planets of iron silicate surface composition, with or without aqueous alteration,[20] unusual materials must be considered. The possibility naturally arises that the strong RED absorption is the signature of a light-harvesting pigment in a photosynthetic system—already suggested, as discussed above, as one possible explanation of the large atmospheric O_2 abundance. Plant life might have to be widespread in order to sustain this O_2 abundance in the face of likely loss by oxidation of the crust. Substantial areas of the surface seem to be covered by this pigment, which on the ground-truth planet is of course chlorophyll *a* and *b*. Photosynthesis might also be driven by oceanic microbes and plants, but the strong red-to-infrared absorption of water makes their pigments much more difficult to detect.

Morphology and topographic resolution

During this fly-by, Galileo's highest resolution systematic imaging of Earth was obtained at 1–2 km per pixel. A two-part mosaic of the ~2,900 by 4,000 km continent of Australia was produced: the eastern half of the continent was imaged mostly with four-band (VIO, GRN, RED, 0.73) coverage at ~1 km per pixel, and the western half with three-band (VIO, GRN, RED) coverage. A mosaic of Antarctica was also produced in three bands (VIO, GRN, RED) at ~2 km per pixel (at the pole).

A later six-band global imaging sequence at ~26 km per pixel showed Australia to be dominated by large central and western deserts, but with some 1.0 μm-bright areas (presumably plant life) concentrated toward the eastern and northern coasts, while Antarctica was found to be almost entirely covered by H_2O ice (Fig. 2*b*). In ~1 km per pixel Galileo mosaics of the Australian continent, no reworking of the surface into geometric patterns, or other compelling indications of artefacts of a technical civilization could be discerned. Although we find some large-scale albedo boundaries in Australian coastal regions that can be associated *a posteriori* with agriculture, in our judgement they are not sufficiently distinctive to be, by themselves, indicative of intelligent life. Kilston *et al.*[21] have demonstrated from a large array of daytime orbital imagery that very few images of the ground-truth Earth at resolution ~1 km reveal evidence of life.

In a study using daytime satellite imaging at 0.1 km resolution, C.S. and Wallace[22] concluded that the chance of finding convincing artifacts in a random frame was only $\sim 10^{-2}$. They further estimated, as a function of resolution, the threshold (in terms of fraction of the ground-truth surface image) for detection of

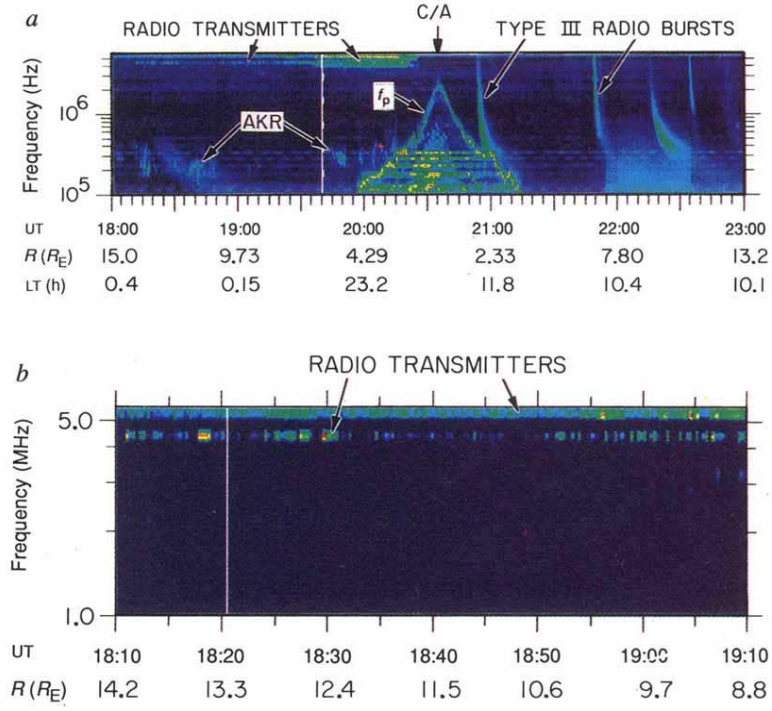

FIG. 4 A frequency–time spectrogram of the radio signals detected by the Galileo plasma wave instrument. The intensities are coded in the sequence blue–green–yellow–red, with blue lowest and red highest. Several natural sources of radio emission are shown in *a*, including auroral kilometric radiation (AKR). Modulated emission at $f > 4$ MHz is shown with an expanded time scale in *b*. Modulated patterns of this type are characteristic of the transmission of information, and would be highly unusual for a naturally occurring radio source. (UT, universal time; *R* is distance of Galileo from Earth in units of Earth's radius, R_E; LT, local time.)

a civilization at the current human level of development (type A) and a hypothetical civilization that reworks its planetary surface to a significantly greater degree (type B). Their Fig. 29 predicts that even with complete surface coverage, detection of a type A civilization would require ~2-km resolution, and type B, ~10-km resolution. Galileo's Australia mosaic represents 2.3% of the whole surface of the Earth imaged at ~1 km per pixel, and the Antarctic mosaic adds another 4% at ~2 km per pixel. Unluckily, these are among the most sparsely settled regions of the ground-truth planet. Imaging about 1% of the surface at this resolution would detect a type B civilization, but imaging nearly all the surface would be required to detect one of type A[22]. A type B civilization is either wholly absent, or present in other continents than Australia and Antarctica. Extensive imaging of the Earth at resolution better than 0.1 km would have readily detected signs of life[23]. The foregoing analysis is based on visible and near-infrared Galileo imaging in reflected sunlight. No usable imaging data were obtained from the night hemisphere of the planet.

Radio emission

Ground-truth television and radar transmissions are predicted to generate a non-thermal radio emission spectrum so strong and striking as to announce the presence of intelligent life not just over interplanetary, but over interstellar distances[24,25]. With a rough knowledge of the composition and structure of the Earth's atmosphere and the solar UV spectrum, it is a straightforward matter[26] to derive the order of magnitude of N_e, the ionospheric electron density in the E and F layers, yielding a plasma frequency f_p ~1–5 MHz. The higher value is the maximum for the sunlit hemisphere. Radio emissions from a technical civilization at the Earth's surface should be detectable only at $f > f_p$.

During the Galileo fly-by, the plasma wave instrument detected radio signals, plausibly escaping through the nightside ionosphere from ground-based radio transmitters. Of all Galileo science measurements, these signals provide the only indication of intelligent, technological life on Earth. They are illustrated in the PWS frequency–time spectrograms in Fig. 4. The transmitter signals can be seen near the top of the spectrograms in Fig. 4*a*, starting at about 18:00 UT and extending to about 20:25 UT, shortly before closest approach (C/A). These signals were detected only during the inbound, nightside pass, and not on the outbound, dayside, pass. Also seen in Fig. 4*a* are a series of Type III solar radio bursts[27] and several bursts of auroral kilometric radiation[28]. The narrow-band emission line labelled f_p is an electrostatic oscillation excited at the local electron plasma frequency by thermal fluctuations in the ionospheric plasma. The sharp peak in f_p near closest approach is caused by the local peak in N_e as the spacecraft passed through the ionosphere at an altitude of ~950 km.

The identification of the narrow-band emissions near 4–5 MHz as ground-based radio transmitters is based on studies by LaBell *et al.*[29] and Keller[30] of the ground-truth planet; satellite observations clearly showed the signals originating from surface transmitters. That a similar conclusion could be drawn from the aforementioned Galileo fly-by data alone, without any previous knowledge of the existence of radio transmitters on Earth, is plausible but not beyond doubt. The rapid increase in the signal strength as the spacecraft approaches the Earth clearly indicates a near-Earth origin. The fact that the signals are only observed on the nightside inbound pass, where the ionosphere propagation cutoff frequency is sufficiently low to allow the signals to escape through the ionosphere, but not on the dayside where the cutoff prevents escape, strongly indicates a source beneath the ionosphere. Taking into account the expected exponential decrease in ionospheric N_e with increasing altitude, the theoretical maximum f_p ~5 MHz is in good agreement with the peak local plasma frequency (~2 MHz) observed at C/A, which was over the sunlit hemisphere at 16:30 LT. (These data might also be consistent with a class of nocturnal transmitting stations orbiting the Earth above the ionosphere, but the conclusion of intelligent life would be unchanged.)

More difficult to estimate from first principles is the nightside f_p, because it depends on various losses and secondary ionization processes that cannot easily be evaluated from Galileo data alone. But because the primary (UV) ionization source is absent on the nightside, it is clear that N_e there will be much lower than on the dayside. From remote observations of Venus and Mars, it is entirely plausible that the nightside f_p should be depressed by factors of three to ten, relative to dayside values, permitting the escape of radio signals through the nightside ionosphere at 4–5 MHz, and providing a consistent overall interpretation of the day–night asymmetry in the observed radio signal. Ground-truth measurements of the night-time ionosphere show that $f_p < 4$ MHz is quite common, particularly at high latitudes[31].

The signals are confined mainly to two or three distinct channels near the top of the spectrogram (Fig. 4). The fact that the central frequencies of these signals remain constant over periods of hours strongly suggests an artificial origin. Naturally generated radio emissions almost always display significant long-term frequency drifts. Even more definitive is the existence of pulse-like amplitude modulation. When the spectrum in Fig. 4*a* is expanded (Fig. 4*b*), the individual narrow-band components can be seen to have a complex modulation pattern. Although the time resolution of the instrument (18.67 s) is inadequate to decode the modulation, such modulation patterns are never observed for naturally occurring radio emissions and implies the transmission of information. On the basis of these observations, a strong case can be made that the signals are generated by an intelligent form of life on Earth.

Conclusions

From the Galileo fly-by, an observer otherwise unfamiliar with the Earth would be able to draw the following conclusions: The planet is covered with large amounts of water present as vapour, as snow and ice, and as oceans. If any biota exists, it is plausibly water-based. There is so much O_2 in the atmosphere as to cast doubt on the proposition that UV photodissociation of water vapour and the escape of hydrogen provide an adequate source. An alternative explanation is biologically mediated photodissociation of water by visible light as the first step in photosynthesis. An unusual red-absorbing pigment that may serve this purpose, corresponding to no plausible mineral, is found widely on land. Methane is detected at ~1 p.p.m., some 140 orders of magnitude higher than the thermodynamic equilibrium value in this oxygen-rich atmosphere. Only biological processes are likely to generate so large a disparity. But how plausible a world covered with carbon-fixing photosynthetic organism, using H_2O as the electron donor and generating a massive (and poisonous) O_2 atmosphere, might be to observers from a very different world is an open question.

Several per cent of the land surface was imaged at a resolution of a few kilometres—entirely in Australia and Antarctica. No unambiguous sign of technological geometrization was found. Narrow-band pulsed amplitude-modulated radio transmission above the plasma frequency strongly suggests the presence of a technological civilization. Most of the evidence uncovered by Galileo would have been discovered by a similar fly-by spacecraft as long ago as about 2 billion (10^9) years. In contrast, modulated narrow-band radio transmissions could not have been detected before this century.

The identification of molecules profoundly out of thermodynamic equilibrium, unexplained by any non-biological process; widespread pigments that cannot be understood by geochemical processes; and modulated radio emission are together evidence of life on Earth without any *a priori* assumptions about its chemistry; 200 g cm^{-2} O_2 is at least suggestive of biology. Negative results in spacecraft exploration of other planets have thus much wider application than merely to

'life as we know it'. Of course putative ecosystems that are only weakly coupled to the surface environment (for example, subsurface[32,33]) are not excluded by such observations.

Surface oceans of liquid water are unique in the Solar System; conceivably this is part of the reason that Earth is the only planet in the Solar System with abundant surface life. Similar spectroscopic methods, although without resolution of the disk, may be useful in examining planets of other stars for indigenous life, as has been suggested for O_2 by Owen.[34] Large filled-aperture or interferometric telescopes intended for investigating extrasolar planets, especially those of terrestrial mass, might incorporate into their design the wavelength range and spectral resolution that has proved useful in the present work. In the radio search for extraterrestrial intelligence (SETI), optimum transmission through interstellar space and plausible planetary atmospheres lies in the 1–3 GHz range, not the MHz range used here.

The Galileo mission constitutes an apparently unique control experiment on the ability of fly-by spacecraft to detect life at various stages of evolutionary development on other worlds in the Solar System. Although a similar opportunity arises in the summer 1999 Earth fly-by of the ESA/NASA Cassini spacecraft on its way to Saturn, there are, because of funding constraints, no plans to observe the Earth with Cassini. Although a great deal more exploration remains to be done before such conclusions can be considered secure, our results are consistent with the hypothesis that widespread biological activity now exists, of all the worlds in this Solar System, only on Earth. □

Received 17 February; accepted 14 September 1993.

1. Carlson, R. W. *et al. Space Sci. Rev.* **60,** 457–502 (1992).
2. Hord, C. W. *et al. Space Sci. Rev.* **60,** 503–530 (1992).
3. Belton, M. J. S. *et al. Space Sci. Rev.* **60,** 413–455 (1992).
4. Gurnett, D. A. *et al. Space Sci. Rev.* **60,** 341–355 (1992).
5. Lederberg, J. *Nature* **207,** 9–13 (1965).
6. Lovelock, J. *Nature* **207,** 568–570 (1965).
7. Lovelock, J. E. *Proc. R. Soc.* B**189,** 167–181 (1975).
8. Sagan, C. *Proc. R. Soc.* B**189,** 143–166 (1975).
9. Carlson, R. W., Arakelian, T. & Smythe, W. D. *Antarct. J. U.S.* (in the press).
10. Drossart, P. J. *et al. Planet. Space Sci.* (submitted).
11. Henderson, L. J. *The Fitness of the Environment: An Inquiry into the Biological Significance of the Properties of Matter* (Peter Smith, Gloucester, Mass., 1913).
12. von Zahn, U., Kumar, R. S., Neimann, H. & Prinn, R. in *Venus* Ch. 13 (eds Hunten, D. M., Colin, L., Donahue, T. M. & Moroz, V. I.) (Univ. of Arizona Press, Tucson, 1983).
13. Owen, T. in *Mars* Ch. 25 (eds Keiffer, H. H., Jakosky, B. M., Snyder, C. W. & Matthews, M. S.) (Univ. of Arizona Press, Tucson, 1992).
14. Walker, J. G. C. *Evolution of the Atmosphere* (Macmillan, New York, 1977).
15. Léger, A., Pirre, M. & Marceau, F. J. *Astr. Astrophys.* (in the press).
16. Lippincott, E. R., Eck, R. V., Dayhoff, M. O. & Sagan, C. *Astrophys. J.* **147,** 753–764 (1967).
17. Chameides, W. L. & Davis, D. D. *Chem. Engng. News* **60,** 38–52 (1992).
18. Hogan, K. B., Hoffman, J. S. & Thompson, A. M. *Nature* **354,** 181–182 (1991).
19. Lewis, J. S. & Prinn, R. G. *Planets and Their Atmospheres* (Academic, New York, 1984).
20. Bowker, D. E., Davis, R. E., Myrick, D. L., Stacy, K. & Jones, W. T. Ref. Publ. No. 1139 (NASA, Washington, 1985).
21. Kilston, S. D., Drummond, R. R. & Sagan, C. *Icarus* **5,** 79–98 (1966).
22. Sagan, C. & Wallace, D. *Icarus* **15,** 515–554 (1971).
23. Sagan, C. *et al.* in *Biology and the Exploration of Mars* Ch. 9 (eds Pittendrigh, C. S., Vishniac, W. & Pearman, J. P. T.) (Natn. Acad. Sci. Washington, 1966).
24. Shklovskii, I. S. & Sagan, C. *Intelligent Life in the Universe* (Holden Day, San Francisco, 1966).
25. Sullivan, W. T., Brown, S. & Wetherill, C. *Science* **199,** 377–388 (1978).
26. Chapman, S. *Proc. phys. Soc.* **43,** 483–501 (1931).
27. Fainberg, J. & Stone, R. G. *Space Sci. Rev.* **16,** 145–188 (1974).
28. Gurnett, D. A. *J. geophys. Res.* **79,** 4227–4238 (1974).
29. LaBelle, J., Trumann, R. A., Boehm, M. H. & Gewecke, K. *Radio Sci.* **24,** 725–737 (1989).
30. Keller, A. thesis, Univ. Iowa (1990).
31. Hines, C. O., Paghis, I., Hartz, T. R. & Fejer, J. A. *Physics of the Earth's Upper Atmosphere* (Prentice Hall, Englewood Cliffs, 1965).
32. Lederberg, J. & Sagan, C. *Proc. Natn. Acad. Sci. U.S.A.* **48,** 1473–1475 (1962).
33. Gold, T. *Proc. natn. Acad. Sci. U.S.A.* **89,** 6045–6049 (1992).
34. Owen, T. in *Strategies for the Search for Life in the Universe* (ed. Papagiannis, M.) 177–185 (Reidel, Dordrecht, 1980).

ACKNOWLEDGEMENTS. We are grateful to W. O'Neil, F. Fanale, T. Johnson, C. Chapman, M. Belton and other Galileo colleagues, as well as W. Sullivan, for encouragement and support; and to J. Lederberg, A. Léger, J. Lovelock, A. McEwen, T. Owen and J. Tarter for comments. This research was supported by the Galileo Project Office, Jet Propulsion Laboratory, NASA and by a grant from NASA's Exobiology Program.

Direct observation of kinesin stepping by optical trapping interferometry

Karel Svoboda*†, Christoph F. Schmidt*‡, Bruce J. Schnapp§ & Steven M. Block*‖

* Rowland Institute for Science, 100 Edwin Land Boulevard, Cambridge, Massachusetts 02142, USA
† Committee on Biophysics, Harvard University, Cambridge, Massachusetts 02138, USA
§ Department of Cell Biology, Harvard Medical School, Boston, Massachusetts 02115, USA

Do biological motors move with regular steps? To address this question, we constructed instrumentation with the spatial and temporal sensitivity to resolve movement on a molecular scale. We deposited silica beads carrying single molecules of the motor protein kinesin on microtubules using optical tweezers and analysed their motion under controlled loads by interferometry. We find that kinesin moves with 8-nm steps.

ENZYMES such as myosin, kinesin, dynein and their relatives are linear motors converting the energy of ATP hydrolysis into mechanical work, moving along polymer substrates: myosin along actin filaments in muscle and other cells; kinesin and dynein along microtubules. Motion derives from a mechanochemical cycle during which the motor protein binds to successive sites along the substrate, in such a way as to move forward on average[1–3]. Whether this cycle is accomplished through a swinging crossbridge, and how cycles of advancement are coupled to ATP hydrolysis, have been the subject of considerable debate[4–6]. *In vitro* assays for motility[7,8], using purified components interacting in well-defined experimental geometries, permit, in principle, measurement of speeds, forces, displacements, cycle timing and other physical properties of individual molecules, using native or mutant proteins[9–14].

Are there steps?

Do motor proteins make characteristic steps? That is, do they move forward in a discontinuous fashion, dwelling for times at

‡ Present address: Department of Physics, University of Michigan, Ann Arbor, Michigan 48109, USA.
‖ To whom correspondence should be addressed.